

Temperature Oscillations, Complex Oscillations, and Elimination of Extraordinary Temperature Sensitivity in the Iodate–Sulfite–Thiosulfate Flow System

Haimiao Liu, Jingxuan Xie, Ling Yuan, and Qingyu Gao*

College of Chemical Engineering, China University of Mining and Technology, Xuzhou 221008 China

Received: June 28, 2009; Revised Manuscript Received: September 6, 2009

Temperature oscillations and complex pH oscillations in the IO_3^- – SO_3^{2-} – $\text{S}_2\text{O}_3^{2-}$ system were observed in a continuously flow stirred tank reactor. During one period of oscillation, the temperature increases rapidly while the pH shows an extremely sharp change. High-amplitude pH oscillations undergo 1^1 complex oscillations (L^S , oscillations with L large peaks and S small peaks per period) to another kind of higher-amplitude regular oscillations upon increasing the concentration of sulfite step by step. Importantly, the longstanding experimental phenomena, the extraordinary temperature sensitivity of oscillatory behavior reported 20 years ago by Rábai and Beck, can be eliminated by premixing of sulfite and sulfuric acid before entering into the reactor, avoiding local acidification, which brings out fluctuation and temperature sensitivity. The temperature oscillations can be understood by taking into account the interaction between thermal effect of various reactions and heat transfer. Experimental observations, both temperature oscillations and 1^1 -type pH oscillations, are reproduced with a four-step Horváth model by addition of an energy-balance equation. This new detailed dynamical behavior would have potential applications in designing complex chemical waves and pH responsive gels with rhythmical motion.

Introduction

The iodate–sulfite system, better known as the Landolt^{1,2} reaction, exhibits both iodide and proton autocatalysis, which displays clock reaction in batch and bistability in open system, but not oscillations. If one adds an appropriate negative feedback, species such as thiosulfate,^{3,4} ferrocyanide,⁵ or thio-urea,⁶ in a continuously flow stirred tank reactor (CSTR), sustained oscillations in pH can be observed in these Landolt-type systems. Also, a wealth of spatiotemporal phenomena in the FIS (ferrocyanide–iodate–sulfite) system,^{7–10} such as spatial bistability, stationary labyrinthine patterns, and self-replicating spots, have been investigated by now. Most recently, De Kepper's group¹¹ has successfully applied an experimental design method to produce chemical Turing patterns, such as stationary hexagonal arrays of spots and parallel strips of pH patterns in the thiourea–iodate–sulfite (TuIS) reaction. In this paper, our attention is focused on the iodate–sulfite–thiosulfate (IST) reaction. The previous studies on the oscillatory behavior of the IST system has been done by Rábai and Beck.^{3,4} They discovered an extremely sharp minimum, large amplitude, and damped oscillations in pH for the closed system and sustained pH oscillations in a CSTR, while an empirical rate law was also suggested to explain both the closed and open phenomena, in which the catalytic effect of thiosulfate on the iodate oxidation of sulfite and the inhibiting effect of sulfite on the oxidation of thiosulfate by iodate were taken into account. Shortly after these two papers, Luo and Epstein¹² reported an article about a general model for pH oscillators, in which they do not question the plausibility of the reaction of iodate–thiosulfate leading to hydrogen sulfite formation but strongly suggest that an appropriate choice of the rate coefficient without the inhibitory effect of hydrogen sulfite might reproduce the nonmonotonic

batch behavior. Recently, we presented the transition from pH waves to iodine waves in the iodate–sulfite–thiosulfate reaction–diffusion system which results from double autocatalysis of proton and iodide.¹³ Most recently, a revised four-step model has been proposed by Horváth,¹⁴ in which the dynamics in both batch and flow experiments is explained without using the cross-catalytic and inhibitory effect of the substrates thiosulfate and sulfite. For the interpretation of the extraordinarily sharp minimum in pH and the batch oligo-oscillations he used the supercatalytic effect of the hydrogen ion on the iodate–sulfite reaction and the different H^+ dependence of the thiosulfate–iodate reaction along with the parallel formation of sulfite and tetrathionate. Also, it is capable of explaining the sustained oscillations in a CSTR system. Although mechanism of the IST system actually may be more complex, possible subsystems include the iodate–sulfite reaction (Landolt reaction),^{1,2,15–17} iodate–iodide reaction (Dushman reaction),^{17–19} thiosulfate–iodate reaction,²⁰ thiosulfate–iodine reaction,^{21,22} tetrathionate–iodine reaction,^{23,24} and tetrathionate–iodate reaction,²⁵ but the simplified model can well reproduce the important characteristics in experiments.

According to Horváth's revised mechanism model, there are two sulfite sources for positive feedback, one pathway is from the continuous input of fresh sulfite reactant and the other from the reproduction of sulfite by iodate–thiosulfate reaction, which depends on the first-order of hydrogen ion concentration,¹⁴ while the thiosulfate oxidized to tetrathionate by iodate, resulting in an increase of pH, provides a negative feedback. Due to such mechanism, complex pH oscillatory behavior may be present in a CSTR.

Temperature can be both a control parameter and a dynamic variable in studying oscillating chemical reactions. First, oscillations can occur in a range of control temperature only. Parameters such as induction period, amplitude, and period of oscillations also depend on temperature. Temperature change may induce transitions from simple limit cycle oscillations to more and more complex

* To whom correspondence should be addressed. E-mail: gaoqy@cumt.edu.cn.

periodic behavior and chaos.^{26,27} Temperature compensation of the oscillatory period in chemical oscillators was also observed^{28–30} in a certain range of temperature. As a control parameter, temperature can be also used to control pattern formation.^{31,32} Second, temperature as a dynamical variable oscillates on heterogeneous catalytic surfaces.^{33–35} Temperature variation measured by means of a NMR–thermometry imaging technique has been used for visualizing the propagation of chemical waves.³⁶ In several autocatalytic reaction systems, considerable temperature changes take place, such as the chlorite–thiosulfate system,^{36,37} ferrous–nitric acid system,³⁷ and hydrogen peroxide–thiosulfate reaction.³⁸ In previous studies,³ the extraordinary temperature sensitivity of the IST system in open conditions was focused. Our experimental interests in the IST system were motivated principally by its multifeedback sources of bisulfite and the temperature sensitivity. As expected, we observed obvious temperature oscillations and complex pH oscillations in a CSTR. At the same time, the extraordinary temperature sensitivity in open conditions was reinvestigated. In this paper, we report our experiment results and model calculation of the IST flow system.

Experimental Section

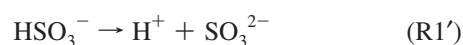
Reagent grade chemicals were used without further purification. Stock solutions of KIO_3 , $\text{Na}_2\text{S}_2\text{O}_3$, Na_2SO_3 , and H_2SO_4 were prepared daily with deionized water (ultrafiltered from Milli-Q system). The flow experiments were performed in a cylinder-shaped CSTR thermostated through a circulating water bath. The plexiglass reactor has a liquid volume of 21 cm^3 . The four chemical solutions saturated with nitrogen for avoiding any effect of O_2 and CO_2 were stored in four separated reservoirs and transferred to CSTR by a high-precision peristaltic pump (ISMATIC). Iodate and thiosulfate solutions entered the CSTR through independent ports, respectively. Sulfite and sulfuric acid feed streams were premixed in a premixing head, just before their entry into the reactor. Excess liquid was removed with an outlet tube. A magnetic stirrer was used to ensure uniform mixing at about 600 rpm. The pH and temperature were simultaneously followed with glass electrode, coupled with a $\text{Hg}|\text{Hg}_2\text{SO}_4|\text{K}_2\text{SO}_4$ reference electrode, and a T-type thermocouple probe (eDAQ) whose signal was amplified through a pH/mV Amp (E165, eDAQ). All signals were collected with a PC computer through an eRecorder (410, eDAQ). During our experiments, it was important that solutions of sulfite and sulfuric acid were premixed before entering into the reactor. This method employed can effectively avoid local acidification.

Results and Discussions

The following reactions R1–R5 are considered here in the IST system. The reversible dissociation of hydrogen sulfite ion (reactions R1 and R1') has a buffering effect, which keeps the pH at the beginning of the reaction around 7.



$$v_1 = k_1[\text{H}^+][\text{SO}_3^{2-}]$$



$$v_{-1} = k_{-1}[\text{HSO}_3^-]$$

The oxidation of hydrogen sulfite by iodate provides a positive feedback of hydrogen ion, the rate equation^{14,39} (v_2) of which

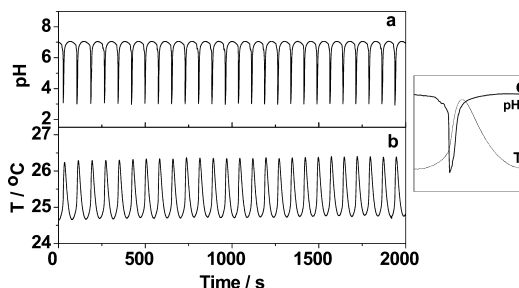
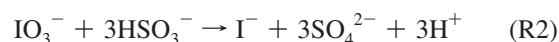


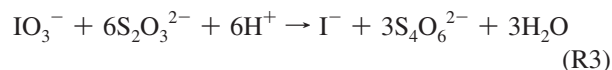
Figure 1. pH and temperature–time series of the IST system in a CSTR. Input concentrations: $[\text{KIO}_3]_0 = 0.075 \text{ mol}\cdot\text{L}^{-1}$, $[\text{H}_2\text{SO}_4]_0 = 0.0383 \text{ mol}\cdot\text{L}^{-1}$, $[\text{Na}_2\text{S}_2\text{O}_3]_0 = 0.0624 \text{ mol}\cdot\text{L}^{-1}$, $[\text{Na}_2\text{SO}_3]_0 = 0.2325 \text{ mol}\cdot\text{L}^{-1}$. $k_0 = 9.52 \times 10^{-3} \text{ s}^{-1}$, $T = 24.7 \text{ }^\circ\text{C}$. The local enlargement (c) on the right shows a oscillatory period of pH and temperature.

contains a term that depends on the square of the concentration of hydrogen ion, making the reaction supercatalytic.



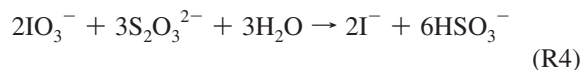
$$v_2 = k_2[\text{HSO}_3^-][\text{IO}_3^-] + k_2'[\text{HSO}_3^-][\text{IO}_3^-][\text{H}^+]^2 + k_2''[\text{HSO}_3^-][\text{IO}_3^-][\text{H}^+]$$

Reaction R3 is the thiosulfate oxidation by iodate, which provides a negative feedback. Its rate equation^{40,41} (v_3) has a second-order dependence on the H^+ concentration.



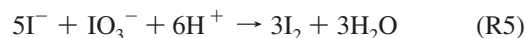
$$v_3 = k_3[\text{S}_2\text{O}_3^{2-}]^2[\text{IO}_3^-][\text{H}^+]^2$$

Hydrogen sulfite is reproduced in step R4, which can open up the route for the R2 step. The rate equation^{14,40,41} of v_4 has a first-order dependence on H^+ concentration. The pH dependence of the parallel oxidation of thiosulfate by iodate into tetrathionate and sulfite has been established experimentally.



$$v_4 = k_4[\text{S}_2\text{O}_3^{2-}][\text{IO}_3^-][\text{H}^+]$$

The well-known Dushman reaction⁴² R5 was considered in closed conditions, since the pH of the solutions decreases below pH 4 at a later stage. However, for most of the time, the value of pH in flow system is above pH 5, leading to the conclusion that the Dushman reaction may be unimportant. Therefore, we neglected this reaction in our mechanistic analysis in a CSTR.



1. Temperature Oscillations. Our systematic investigations have revealed that temperature oscillations occur in a rather wide range of experimental conditions, such as input concentrations, flow rates, and temperatures. The curves shown in Figure 1 are typical time series of temperature and pH observed in a CSTR. As it appears from the curves of Figure 1b, there is an amplitude of more than $1 \text{ }^\circ\text{C}$ in the oscillations in temperature, and the curves of Figure 1a show corresponding pH oscillations with

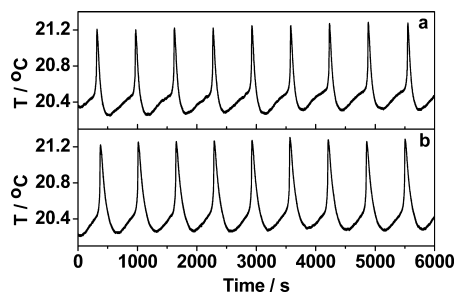


Figure 2. Measured temperature vs time curves of the IST system with thermostating at 20.2 °C (a) and without thermostating at room temperature (20.2 °C) (b), respectively. Input concentrations: $[\text{KIO}_3]_0 = 0.050 \text{ mol}\cdot\text{L}^{-1}$, $[\text{H}_2\text{SO}_4]_0 = 0.021 \text{ mol}\cdot\text{L}^{-1}$, $[\text{Na}_2\text{S}_2\text{O}_3]_0 = 0.0416 \text{ mol}\cdot\text{L}^{-1}$, $[\text{Na}_2\text{SO}_3]_0 = 0.1583 \text{ mol}\cdot\text{L}^{-1}$, $k_0 = 9.52 \times 10^{-4} \text{ s}^{-1}$.

high frequency and large amplitude. The character of oscillations depends very much on the reactants concentration. Small amplitude of about 0.2 °C of the temperature oscillations can be observed at the same conditions in Figure 2 except $[\text{H}_2\text{SO}_4]_0 = 0.0266 \text{ mol}\cdot\text{L}^{-1}$, $[\text{Na}_2\text{SO}_3]_0 = 0.100 \text{ mol}\cdot\text{L}^{-1}$. Temperature oscillations show the same character at room temperature (20.2 °C) and water-jacketed temperature (20.2 °C) (Figure 2a,b). We also investigated changes of the amplitude and period by varying sulfite concentration, flow rate, and temperature, respectively, as other parameters were fixed. Figure 3a shows that the amplitude of temperature oscillations linearly increases with the sulfite concentration, as does the period. The maximum amplitude can be higher than 1 °C. Furthermore, increasing the concentration of thiosulfate leads to the increased amplitude of temperature oscillations, but amplitude was decreased when increasing the concentration of sulfuric acid and iodate, respectively. To summarize, sulfite has the largest effect on the temperature oscillations, sulfuric acid and iodate have the second greatest effect, and thiosulfate has the least. The amplitude decreases while the period increases as the flow rate is reduced, as illustrated in Figure 3b, but the relationship between period and flow rate is nonlinear. Both the amplitude and period decrease linearly as the temperature increased (Figure 3c), but the change in them is small for both.

The temperature oscillations can be understood as follows: reactions with fast rate and exothermic character make the temperature of the system increase, since the heat released cannot be exchanged with the circulated water immediately; then slow reaction process make the temperature drop due to the heat well exchanged between the reactor and the circulated water. R2–R4 are exothermic reactions. During a period of oscillation, as shown in Figure 1c, the temperature increases quickly while the pH shows an extremely sharp drop and rise, which results from the exothermic reactions of the fast oxidation of sulfite and thiosulfate by iodate. During these processes, released heat could not be immediately exchanged with the circular water, which caused a rise of temperature. In contrast, at high pH for a long time with slow R4, the heat released was exchanged with the circular water bath, leading to a temperature drop until the pH dropped again, and the temperature cycle starts again.

2. Eliminating Extraordinary Temperature Sensitivity of Oscillatory Behavior by Premixing. In previous studies, the extraordinary temperature sensitivity of the system in open conditions was the focus. Rábai and Beck^{3,4} found that below 18 °C and above 22 °C in thermostatic water there was no oscillatory behavior at the given initial concentrations and flow rate, and the period had tripled from 21 to 20 °C. When the initial concentrations of the reactants were twice the concentrations given in Figure 2 of the paper,³ the oscillations stopped

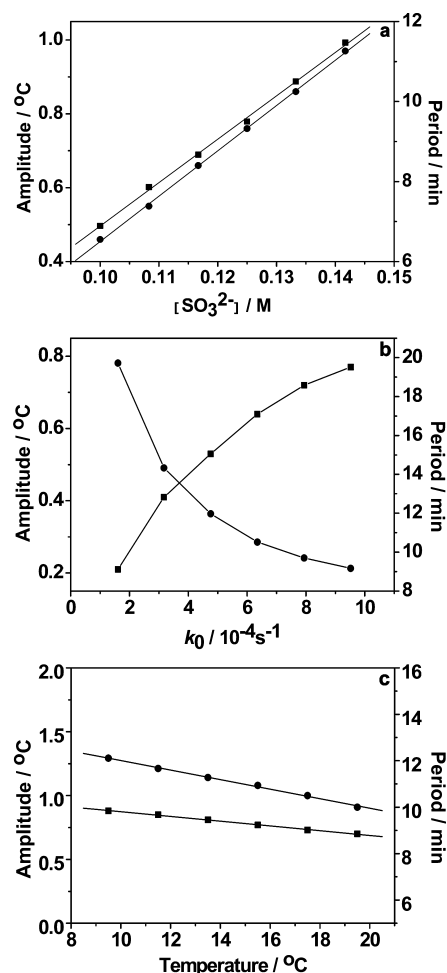


Figure 3. The amplitude and period of the temperature oscillations as a function of the concentration of sulfite (a), flow rate (b), and temperature (c), respectively. (●) period, (■) amplitude. Input concentrations: $[\text{KIO}_3]_0 = 0.050 \text{ mol}\cdot\text{L}^{-1}$, $[\text{H}_2\text{SO}_4]_0 = 0.021 \text{ mol}\cdot\text{L}^{-1}$, $[\text{Na}_2\text{S}_2\text{O}_3]_0 = 0.0416 \text{ mol}\cdot\text{L}^{-1}$, $[\text{Na}_2\text{SO}_3]_0 = 0.1267 \text{ mol}\cdot\text{L}^{-1}$ (b, c), $k_0 = 9.52 \times 10^{-4} \text{ s}^{-1}$ (a, c). $T = 20.0 \text{ °C}$ (a, b).

after a few periods. They believed that without particularly intensive and careful thermostating, the rather exothermic nature of the reaction led to a continuous stepwise increase of the temperature in the reactor, which led soon to the ceasing of the oscillations. In our experiments, the oscillatory behavior in the flow system is not extraordinarily sensitive to temperature. With circulation water from 40 to 5 °C, oscillatory behaviors were sustained at the given initial concentrations: $[\text{KIO}_3]_0 = 0.025 \text{ mol}\cdot\text{L}^{-1}$, $[\text{Na}_2\text{SO}_3]_0 = 0.05 \text{ mol}\cdot\text{L}^{-1}$, $[\text{Na}_2\text{S}_2\text{O}_3]_0 = 0.0208 \text{ mol}\cdot\text{L}^{-1}$, $[\text{H}_2\text{SO}_4]_0 = 0.0105 \text{ mol}\cdot\text{L}^{-1}$, at the flow rate of $k_0 = 9.52 \times 10^{-4} \text{ s}^{-1}$. As Figure 4 shows, the period of oscillations has gradually small change in the range of temperatures (26–16 °C). Although the reactions in the IST system are essentially exothermic, a heat exchange can be obtained by the well-controlled thermostating of water during an oscillatory period. Just because of this, when the initial concentrations of the reactants were 2-, 4-, or 6-fold of the concentrations $[\text{KIO}_3]_0 = 0.0125 \text{ mol}\cdot\text{L}^{-1}$, $[\text{Na}_2\text{SO}_3]_0 = 0.025 \text{ mol}\cdot\text{L}^{-1}$, $[\text{Na}_2\text{S}_2\text{O}_3]_0 = 0.0104 \text{ mol}\cdot\text{L}^{-1}$, $[\text{H}^+]_0 = 0.0105 \text{ mol}\cdot\text{L}^{-1}$, the oscillations were sustained in a wide range of flow rate and temperature. To compare experimental methods used in the study of Rábai and Beck³ and this paper, the four solutions (potassium iodate, sodium sulfite, sodium thiosulfate, and sulfuric acid) were pumped into the reactor, but in our experiments, solutions of sulfite and sulfuric acid were premixed before entering into the reactor. During the

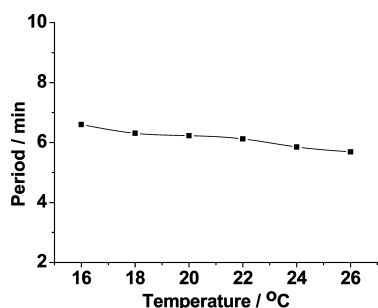


Figure 4. The period of pH oscillations as a function of the temperature. Input concentrations: $[\text{IO}_3^-]_0 = 0.050 \text{ mol}\cdot\text{L}^{-1}$, $[\text{S}_2\text{O}_3^{2-}]_0 = 0.0416 \text{ mol}\cdot\text{L}^{-1}$, $[\text{H}_2\text{SO}_4]_0 = 0.021 \text{ mol}\cdot\text{L}^{-1}$, $[\text{SO}_3^{2-}]_0 = 0.100 \text{ mol}\cdot\text{L}^{-1}$, $k_0 = 9.52 \times 10^{-4} \text{ s}^{-1}$.

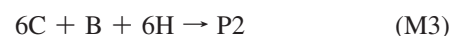
reaction process, sulfuric acid through a single channel to the reactor would make local acidification in the reaction mixture. Since all reactions in the IST system have different dependence on the proton and all are exothermic reactions, a local high concentration of hydrogen ion leads to fast reaction and a temperature rise in local area that results in the temperature sensitivity of the oscillatory behavior. Further, local acidification in Rábai's method could not be avoided, even though the stirring rate was over 1000 rpm. As bromothymol blue, a pH color indicator that switches from blue to yellow in the 7.6–6.0 pH range, was added into the reservoir of sulfuric acid and then pumped it to the reactor, we found local yellow in close vicinity to the port. Premixing sulfite and sulfuric acid can effectively avoid local acidification due to the protonation equilibrium between sulfite and bisulfite, so the extreme temperature sensitivity of the oscillatory behavior was eliminated in our experiments.

3. Complex pH Oscillations. With increasing sulfite concentration step by step, high amplitude simple pH oscillations went through 1^1 -type sequences to another kind of higher-amplitude regular oscillations in this chemical system. Results shown in Figure 5 are typical pH–time series at different sulfite concentrations in a CSTR. One can see that two small peaks in high pH change alternatively when increasing the sulfite concentration. The second small peak began to form when the sulfite concentration was $0.120 \text{ mol}\cdot\text{L}^{-1}$ (Figure 5b) and then it grew gradually from small to big (Figure 5c–e), but meanwhile, the first peak weakened (Figure 5a–d) and then disappeared when the sulfite concentration was $0.1556 \text{ mol}\cdot\text{L}^{-1}$ (Figure 5e). The oscillations were transformed to larger-amplitude and longer-period pH oscillations in Figure 5e with higher sulfite concentration compared with Figure 5a; the amplitude of pH is over 4, and obviously the pH maximum dropped. Influences of concentrations of sulfuric acid, thiosulfate, iodate, flow rate, and temperature on the peculiar phenomena are also investigated, respectively. With the concentration of sulfuric acid decreased, there is similar behavior with increasing the concentration of sulfite, but other parameter changes cannot make this exotic behavior visible in our study.

During a period of oscillation, the pH is around 7.7 at the beginning of the reaction, resulting from the buffering effect of the hydrogen sulfite–sulfite system. A sharp drop in pH occurs because of the autocatalytic R2 reaction after the buffer capacity is exhausted, then it shows an increase in pH due to reaction R3. From the rate equations of v_3 and v_4 , one can notice that the two processes have different dependence on the concentration of H^+ : the tetrathionate pathway has a second-order dependence on H^+ , while sulfite pathway has a first order H^+ dependence. Therefore, at lower pH the tetrathionate formation is preferred, and at higher pH, hydrogen sulfite reproduction is

most likely to be the dominant one. There are two parallel origins of hydrogen sulfite for positive feedback, resulting in the 1^1 -type pH oscillations, one is derived from reaction R4 and the other from the input flow of sulfite. In the experimental condition of Figure 5a, the pH–time curve of one period can be divided into three stages: from point I to II, the dominant reaction of the stage is proton autocatalysis R2. At point II, all the bisulfite that results from input flow and R4 has been consumed. Reaction R3 comes to play from point II until point III in Figure 5a. Then a small pH drop originates from R4 and R2, in which hydrogen sulfite is reproduced from R4 and is consumed in R2, until the continuous input of the reactants causes the autocatalytic oxidation of bisulfite by iodate to begin the next cycle. As can be clearly seen from Figure 5b–d, the effect of the increased input sulfite concentration makes the pH rise again (from point IV to point I in Figure 5c), leading to the second peak that appears and then grows bigger. As the input sulfite concentration increased to $0.1556 \text{ mol}\cdot\text{L}^{-1}$, its effect is dominant while the effect of R4 is weak during the stage from point III to I (illustrated in Figure 5c), which results in the first small peak disappearing and the second peak being the biggest. In addition, the amplitude becomes bigger and the minimum pH of oscillations drops under 4 by increasing the input concentration of sulfite (Figure 5e) since R2 reaction autocatalytically produces more H^+ . Because increased sulfite concentration consumed more iodate in reaction R2, the decreased iodate left for reaction R3 results in deceleration of this step, leading to the slow pH rise in Figure 5e.

4. Model and Simulation. We attempted to simulate the temperature oscillations and complex pH oscillations of the IST system by the four-step Horváth model¹⁴ and the energy-balance equation⁴³ with the stiff method of the Berkeley Madonna program.⁴⁴ The kinetic model suggested was given as follows:



where A, B, C, and H stand for sulfite, iodate, thiosulfate, and hydrogen ions, and P1 and P2 correspond to sulfate and tetrathionate, respectively. The following rate equations were considered:

$$v_{\text{M1}} = k_{\text{M1}}[\text{H}][\text{A}]v_{-\text{M1}} = k_{-\text{M1}}[\text{HA}] \quad (1)$$

$$v_{\text{M2}} = k_{\text{M2}}[\text{HA}]^2[\text{B}] + k_{\text{M2}}'[\text{HA}][\text{B}][\text{H}]^2 + k_{\text{M2}}''[\text{HA}][\text{B}][\text{H}] \quad (2)$$

$$v_{\text{M3}} = k_{\text{M3}}[\text{C}]^2[\text{B}][\text{H}]^2 \quad (3)$$

$$v_{\text{M4}} = k_{\text{M4}}[\text{C}][\text{B}]^2[\text{H}] \quad (4)$$

The energy-balance equation can be written as

$$c_p \sigma \frac{dT}{dt} = c_p \sigma k_0 (T - T_0) + \sum_i \Delta H_i v_i - \frac{\chi S (T - T_a)}{V} \quad (5)$$

where c_p is the specific heat capacity of liquid water, σ the density, χ the surface heat transfer coefficient, S the surface area, V the

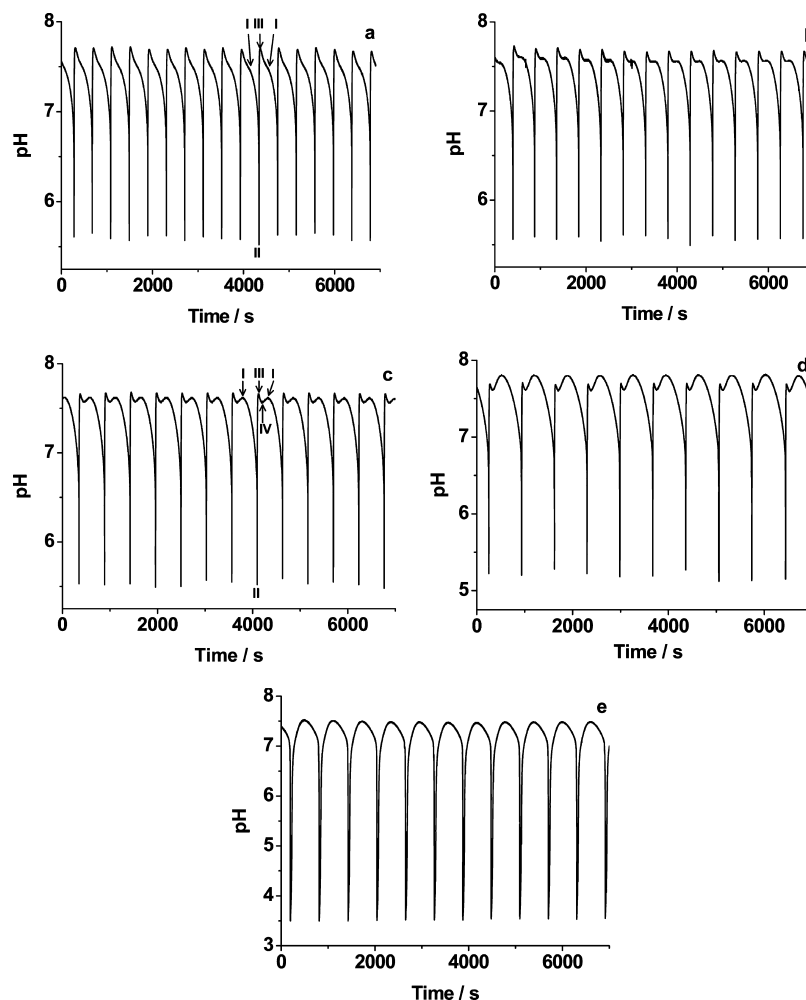


Figure 5. Measured pH vs time curves at different concentration of sulfite in a CSTR. Input concentrations: $[\text{KIO}_3]_0 = 0.050 \text{ mol}\cdot\text{L}^{-1}$, $[\text{H}_2\text{SO}_4]_0 = 0.021 \text{ mol}\cdot\text{L}^{-1}$, $[\text{Na}_2\text{S}_2\text{O}_3]_0 = 0.0416 \text{ mol}\cdot\text{L}^{-1}$. $[\text{Na}_2\text{SO}_3]_0$ varied as follows: (a) $0.1067 \text{ mol}\cdot\text{L}^{-1}$, (b) $0.120 \text{ mol}\cdot\text{L}^{-1}$, (c) $0.1267 \text{ mol}\cdot\text{L}^{-1}$, (d) $0.1389 \text{ mol}\cdot\text{L}^{-1}$, and (e) $0.1556 \text{ mol}\cdot\text{L}^{-1}$. $k_0 = 9.52 \times 10^{-4} \text{ s}^{-1}$. $T = 20 \text{ }^\circ\text{C}$.

reactor volume, T_0 the inflow temperature, and T_a the ambient temperature in which the reactor is sitting. v_i and ΔH_i are the rate law and molar reaction enthalpy for each reaction. The values of c_p , σ , χ , S are $4.18 \times 10^{-3} \text{ kJ}\cdot\text{g}^{-1}\cdot\text{K}^{-1}$, $998.20 \text{ g}\cdot\text{L}^{-1}$, $149.36 \text{ kJ}\cdot\text{m}^{-2}\cdot\text{s}^{-1}\cdot\text{K}^{-1}$, and $4.52 \times 10^{-3} \text{ m}^2$, respectively. In calculations, there are six variables including A, B, C, H, HA and the temperature of the reaction system in a CSTR.

$$\frac{d[A]}{dt} = -v_{M1} + v_{-M1} + k_0([A]_0 - [A]) \quad (6)$$

$$\frac{d[B]}{dt} = -v_{M2} - v_{M3} - 2v_{M4} + k_0([B]_0 - [B]) \quad (7)$$

$$\frac{d[C]}{dt} = -6v_{M3} - 3v_{M4} + k_0([C]_0 - [C]) \quad (8)$$

$$\frac{d[H]}{dt} = -v_{M1} + v_{-M1} + 3v_{M2} - 6v_{M3} + k_0([H]_0 - [H]) \quad (9)$$

$$\frac{d[\text{HA}]}{dt} = v_{M1} - v_{-M1} - 3v_{M2} + 6v_{M4} - k_0[\text{HA}] \quad (10)$$

$$\frac{dT}{dt} = \frac{-H_{M1}v_{M1} - H_{-M1}v_{-M1} - H_{M2}v_{M2} - H_{M3}v_{M3} - H_{M4}v_{M4}}{c_p\sigma} + k_0(T - T_0) - \frac{\chi S(T - T_a)}{c_p\sigma V} \quad (11)$$

In the system, the forward reaction of M1 is exothermic and the reverse one is endothermic; the molar reaction enthalpy is $\pm 9.28 \text{ kJ/mol}$. The M2, M3, and M4 reactions are all exothermic; the molar reaction enthalpy of them are -684.84 , -452.73 , and -613.89 kJ/mol , respectively. The formation enthalpies of each species were obtained from *Lange's Chemistry Handbook*.⁴⁵ Since the temperature change is only more than $1 \text{ }^\circ\text{C}$, here the temperature effect of all rate coefficients is neglected. So the rate constants used here are the same as in the literature.¹⁴

Shown in Figure 6 are typical calculated pH and temperature-time series. Simulations show that the drop of pH occurred while the temperature increased rapidly, due to the heat released from the oxidation of sulfite by iodate, then the temperature decreased as the pH increased slowly, which is consistent with the experimental results when the sulfite concentration is high. The calculated curves are much sharper than that found in the experiments. It probably requires the improvement of the kinetic model along with the energy balance equation.

Figure 6a2 is the calculated 1^1 -type pH oscillations transitioned from simple oscillations (Figure 6a1) as sulfite concentration is increased. Comparing with the pH oscillations, the amplitude of the small peak of 1^1 -type temperature oscillations is too small to be observed unless they are enlarged, as shown in the inset of Figure 6b2. Therefore, the similar small temperature peak in experiments cannot be observed. We also found the 1^2 , 1^n ($n \geq 3$) oscillations in the calculation by varying the flow rate. These

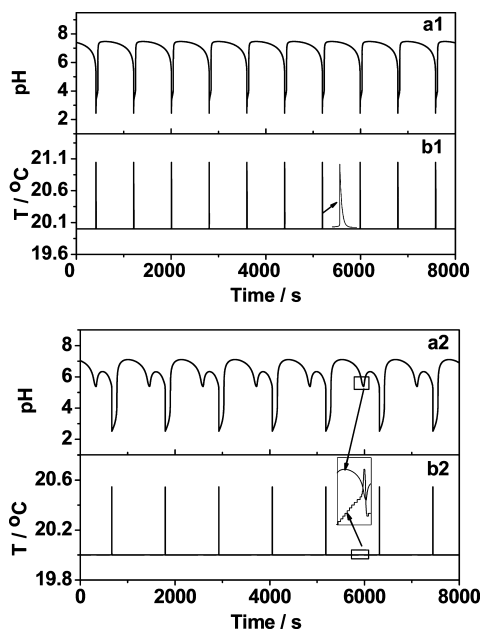


Figure 6. Calculated pH and temperature–time series on the basis of rate eqs 1–5 at the initial different sulfite concentration in a CSTR. Rate coefficients: $k_{M1} = 10^{11} \text{ M}^{-1} \cdot \text{s}^{-1}$, $k_{-M1} = 10^4 \text{ s}^{-1}$, $k_{M2} = 20 \text{ M}^{-2} \cdot \text{s}^{-1}$, $k_{M2'} = 4.7 \times 10^{10} \text{ M}^{-3} \cdot \text{s}^{-1}$, $k_{M2''} = 8800 \text{ M}^{-2} \cdot \text{s}^{-1}$, $k_{M3} = 1.3 \times 10^{12} \text{ M}^{-3} \cdot \text{s}^{-1}$, $k_{M4} = 4.6 \times 10^6 \text{ M}^{-3} \cdot \text{s}^{-1}$. $[\text{IO}_3^-]_0 = 0.050 \text{ mol} \cdot \text{L}^{-1}$, $[\text{Na}_2\text{S}_2\text{O}_3]_0 = 0.0416 \text{ mol} \cdot \text{L}^{-1}$, $[\text{H}^+]_0 = 0.0261 \text{ mol} \cdot \text{L}^{-1}$; $[\text{Na}_2\text{SO}_3]_0 = 0.111 \text{ mol} \cdot \text{L}^{-1}$ (1) or $0.1212 \text{ mol} \cdot \text{L}^{-1}$ (2). $k_0 = 9.52 \times 10^{-4} \text{ s}^{-1}$. $T = 20.0 \text{ }^\circ\text{C}$. The insets show enlarged temperature and pH curves during a period.

calculations have revealed that this phenomenon can only be found in a very narrow flow rate range. Similar characteristics were also observed by varying separately the initial concentration of the reactants in a narrow range. Unfortunately, we have not found this kind of complex oscillation in experiments.

Conclusion

As we expected, temperature oscillations and complex 1¹-type pH oscillations were observed in the IST flow system. Temperature oscillations result from the interaction between exothermic reactions and heat transfer. Complex pH oscillations are the consequence of the competitive positive feedbacks for hydrogen sulfite; one of the pathways reproduces hydrogen sulfite through reaction R4, the other is from the input flow of sulfite. Sustained temperature and pH oscillations were present at a broad range of temperatures and reagent concentrations. The period of pH oscillations experienced a gradual small change in the experimental temperature range. Extraordinary temperature sensitivity of oscillatory dynamics in a CSTR can be eliminated through premixing sulfite and sulfuric acid before entering the reactor, which effectively avoids local acidification in the reaction mixture. Compared with a previous report³ in which four solutions of the IST system entered the reactor through independent ports, the extreme temperature sensitivity may be attributed to unavoidable local acidification. In addition, the combination of a four-step Horváth model and an energy balance equation could simulate temperature oscillations and 1¹-type pH oscillations. This experimental investigation of the IST system in flow conditions provides the further understanding

of the mechanism and the possibility of new reaction–diffusion phenomena in the media of complex oscillations.

Acknowledgment. This work was supported by the NSFC (Grant 20810402063), NCET (Grant 05-0477), and JSNSF (BK2007037). We are grateful to Mr. Gengli Zhang for the reactor design.

References and Notes

- (1) Landolt, H. *Ber. Drsch. Chem. Ges.* **1886**, *19*, 1317.
- (2) Eggert, J.; Scharnow, B. *Z. Electrochem. Angew. Phys. Chem.* **1921**, *27*, 455.
- (3) Rábai, G.; Beck, M. T. *J. Phys. Chem.* **1988**, *92*, 2804.
- (4) Rábai, G.; Beck, M. T. *J. Phys. Chem.* **1988**, *92*, 4831.
- (5) Edblom, E. C.; Orbán, M.; Epstein, I. R. *J. Am. Chem. Soc.* **1986**, *108*, 2826.
- (6) Rábai, G.; Nagy, V. Zs.; Beck, M. T. *React. Kinet. Catal. Lett.* **1987**, *33*, 23.
- (7) Szalai, I.; De Kepper, P. *Chaos* **2008**, *18*, 026105.
- (8) Lee, K. J.; McCormick, W. D.; Ouyang, Q.; Swinney, H. L. *Science* **1993**, *261*, 192.
- (9) Lee, K. J.; McCormick, W. D.; Pearson, J. E.; Swinney, H. L. *Nature* **1994**, *369*, 215.
- (10) Li, G.; Ouyang, Q.; Swinney, H. L. *J. Chem. Phys.* **1996**, *105*, 10830.
- (11) Horváth, J.; Szalai, I.; De Kepper, P. *Science* **2009**, *324*, 772.
- (12) Luo, Y.; Epstein, I. R. *J. Am. Chem. Soc.* **1991**, *113*, 1518.
- (13) Gao, Q. Y.; Xie, R. Y. *Chem. Phys. Chem.* **2008**, *9*, 1153.
- (14) Horváth, A. K. *J. Phys. Chem. A* **2008**, *112*, 3935.
- (15) Gáspár, V.; Showalter, K. *J. Am. Chem. Soc.* **1987**, *109*, 4869.
- (16) Horváth, A. K.; Nagypál, I.; Csekő, G. *J. Phys. Chem. A* **2008**, *112*, 7868.
- (17) Csekő, G.; Varga, D.; Horváth, A. K.; Nagypál, I. *J. Phys. Chem. A* **2008**, *112*, 5954.
- (18) Xie, Y.; McDonald, M. R.; Margerum, D. W. *Inorg. Chem.* **1999**, *38*, 3938.
- (19) Schmitz, G. *Phys. Chem. Chem. Phys.* **2000**, *2*, 4041.
- (20) Rieder, R. *J. Phys. Chem.* **1930**, *34*, 2111.
- (21) Awtrey, A. D.; Connick, R. E. *J. Am. Chem. Soc.* **1951**, *73*, 1341.
- (22) Scheper, W. M.; Margerum, D. W. *Inorg. Chem.* **1992**, *31*, 5466.
- (23) Awtrey, A. D.; Connick, R. E. *J. Am. Chem. Soc.* **1951**, *73*, 4546.
- (24) Kerek, A.; Horváth, A. K. *J. Phys. Chem. A* **2007**, *111*, 4235.
- (25) Koh, T.; Yajima, M. *Bull. Chem. Soc. Jpn.* **1991**, *64*, 1854.
- (26) Orbán, M.; Epstein, I. R. *J. Phys. Chem.* **1982**, *86*, 3907.
- (27) Rábai, G.; Szántó, T. G.; Kovács, K. *J. Phys. Chem. A* **2008**, *112*, 12007.
- (28) Rábai, G.; Hanazaki, I. *Chem. Commun.* **1999**, 1965.
- (29) Kovács, K. M.; Rábai, G. *Phys. Chem. Chem. Phys.* **2002**, *4*, 5265.
- (30) Kovács, K. M.; Hussami, L. L.; Rábai, G. *J. Phys. Chem. A* **2005**, *109*, 10302.
- (31) Mair, T.; Warnke, C.; Tsuji, K.; Müller, S. C. *Biophys. J.* **2005**, *88*, 639.
- (32) McIlwaine, R.; Vanagw., V. K.; Epstein, I. R. *Phys. Chem. Chem. Phys.* **2009**, *11*, 1581.
- (33) Hu, Y. H.; Ruckenstein, E. *Ind. Eng. Chem. Res.* **1998**, *37*, 2333.
- (34) Bychkov, V. Y.; Tyulenim, Y. P.; Slinko, M. M.; Korchak, V. N. *Appl. Catal. A: Gen.* **2007**, *321*, 180.
- (35) Bychkov, V. Y.; Tyulenim, Y. P.; Slinko, M. M.; Korchak, V. N. *Surf. Sci.* **2009**, *603*, 1680.
- (36) Zhivonitko, V. V.; Koptuyug, I. V.; Sagdeev, R. Z. *J. Phys. Chem. A* **2007**, *111*, 4122.
- (37) Nagypál, I.; Bazsa, G.; Epstein, I. R. *J. Am. Chem. Soc.* **1986**, *108*, 3635.
- (38) Chang, M.; Schmitz, R. A. *Chem. Eng. Sci.* **1975**, *30*, 21.
- (39) Skrabal, A.; Zahorka, A. *Z. Electrochem. Angew. Phys. Chem.* **1927**, *33*, 42.
- (40) Rieder, R. *J. Phys. Chem.* **1930**, *34*, 2111.
- (41) Indelli, A. *J. Phys. Chem.* **1961**, *65*, 240.
- (42) Dushman, S. J. *J. Phys. Chem.* **1904**, *8*, 453.
- (43) Scott, S. K. *Chemical Chaos*; Clarendon Press: Oxford, U.K., 1991, p 89.
- (44) <http://www.berkeleymadonna.com/>.
- (45) Dean, J. A., Ed. *Lange's Handbook of Chemistry*, 15th ed.; McGraw-Hill, New York, 1999.